

Crystal Structure of a Lightweight Borohydride from Submicrometer Crystallites by Precession Electron Diffraction

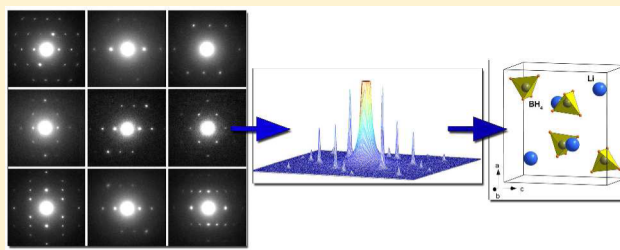
Joke Hadermann,^{*,†} Artem Abakumov,[†] Senne Van Rompaey,[†] Tyché Perkisas,[†] Yaroslav Filinchuk,[‡] and Gustaaf Van Tendeloo[†]

[†]EMAT, University of Antwerp, Groenenborgerlaan 171, 2020 Antwerp, Belgium

[‡]Institute of Condensed Matter and Nanosciences, Université Catholique de Louvain, Place L. Pasteur 1, B-1348 Louvain-la-Neuve, Belgium

S Supporting Information

ABSTRACT: We demonstrate that precession electron diffraction at low-dose conditions can be successfully applied for structure analysis of extremely electron-beam-sensitive materials. Using LiBH_4 as a test material, complete structural information, including the location of the H atoms, was obtained from submicrometer-sized crystallites. This demonstrates for the first time that, where conventional transmission electron microscopy techniques fail, quantitative precession electron diffraction can provide structural information from submicrometer particles of such extremely electron-beam-sensitive materials as complex lightweight hydrides. We expect the precession electron diffraction technique to be a useful tool for nanoscale investigations of thermally unstable lightweight hydrogen-storage materials.



KEYWORDS: electron diffraction, precession, borohydride, LiBH_4 , electron microscopy

1. INTRODUCTION

Hydrogen is one of the most promising mediums for ecologically clean energy storage and transportation. Complex hydrides of lightweight elements, such as NaAlH_4 and LiBH_4 , are extensively discussed as materials for reversible hydrogen release/uptake.¹ LiBH_4 , one of the lightest known complex hydrides, contains 18.5 wt % hydrogen compared to 7.4 wt % in NaAlH_4 . From this 18.5 wt %, only up to 5.6 wt % can be extracted reversibly at reasonable temperatures. Although LiBH_4 demonstrates a higher hydrogen content, it has an unfavorable high thermal stability in the hydrogen-release process.^{2,3} However, adding third components to the system in order to improve the thermodynamic and/or kinetic aspects shows promising results. For example, adding MgH_2 to LiBH_4 decreases the enthalpy of the decomposition process by ~ 25 kJ/mol because of the formation of stable MgB_2 as a byproduct.⁴ Also, titanium-based species [$\text{Ti}(\text{O-butyl})_4$, TiCl_3 , or titanium nanoparticles] used as catalysts provide an enhancement of more than 1 order of magnitude on the hydrogenation/dehydrogenation rate in NaAlH_4 .⁵ The clear tendency to depart from single-phase hydrides toward more complex composite systems requires an understanding of the interactions between the constituents of such composites. Often these systems achieve extra benefit from the nanoscale mixing of the components;⁴ therefore, spatially localized information on the hydrogenation/dehydrogenation products and intermediates can have a significant impact on the further improvement of their performance. In principle, transmission

electron microscopy (TEM) is by far the best method to obtain such structural and chemical information with a resolution down to the atomic level. However, the applicability of TEM to lightweight complex hydrides is commonly recognized as extremely challenging. Although direct imaging of the H atoms was demonstrated for YH_2 , this unique example cannot be correlated with the general situation in lightweight complex hydrides. YH_2 is known as one of the most thermodynamically stable hydrides even under low pressures and shows moderate stability toward electron-beam irradiation.⁶ The low thermal stability (required for hydrogen-storage application) of other lightweight metal hydrides drastically increases their decomposition by electron-beam heating in the vacuum of the microscope. Another important mechanism is the “knock-on” damage, i.e., damage caused by high-energy electrons transferring their kinetic momentum to the nuclei, knocking them out of their site and creating a vacancy-interstitial pair. The lower the atomic number of an element, the more prone it is to “knock-on” damage. In combination with the low thermal stability, this makes the lightweight complex hydrides seemingly hopeless objects for TEM investigations. Decreasing the kinetic energy of the electrons by decreasing the operating accelerating voltage could be a solution, but for B atoms, the threshold of the “knock-on” damage is below 80 kV, while for the lighter Li

Received: May 19, 2012

Revised: August 1, 2012

Published: August 1, 2012

and H atoms, it drops below 60 kV, where commercial TEM instruments do not yet operate.⁷ Also, it was demonstrated that lowering the accelerating voltage to 100 kV and cooling a NaAlH₄ sample down to liquid-N₂ temperature do not improve the stability under the electron beam.⁸ Moreover, even though lowering the voltage reduces the “knock-on” damage, it increases the heating by the electron beam, which is equally harmful for borohydrides during TEM observations. Lowering the electron dose is suggested as the only solution,⁹ but atomic-scale imaging techniques such as high-resolution transmission electron microscopy (HRTEM) and high-angle annular dark-field scanning transmission electron microscopy (HAADF-STEM) require a high signal-to-noise ratio and cannot be performed at the low-dose conditions necessary for lightweight complex hydrides to survive. Thus, for example, on NaAlH₄, TEM images can only be taken at size scales that do not allow the retrieval of any atomic-scale information.^{8,10}

When real-space imaging damages the material, working in reciprocal space can offer a valuable alternative because electron diffraction (ED) requires a significantly lower electron dose. Selected-area electron diffraction (SAED) already provides valuable crystallographic information (interplanar spacings, unit cell, and space group), which can be used for phase identification, but it is not applicable for solving the atomic structure because of the intrinsic dynamic nature of the electron–matter interaction. However, using precession electron diffraction (PED) significantly reduces the unwanted intensity distortions from dynamic scattering by diminishing the number of simultaneously excited diffracted beams.¹¹ PED was, for example, successfully applied for the crystal structure determination of Li₂CoPO₄F, suffering from moderate beam damage (HAADF-STEM and HRTEM images could also be taken, but the material rapidly becomes amorphous under the beam).¹² To our knowledge, the smallest crystal used for PED data collection, structure solution, and refinement was a SrP₃N₅O nanorod with a size of 80 nm × 20 nm × 1000 nm.¹³ Quantitative PED intensities can be collected from even smaller crystals, as was demonstrated for the 3–5 nm precipitates of Mg₂Zn_{5-x}Al_{2+x} within an aluminum matrix. However, the quality of these data is not superior, allowing structure analysis with the Patterson method, but excluding structure refinement.¹⁴ PED patterns collected on the scale of 2–3 nm were used only for phase analysis (phase mapping) based on a qualitative comparison of the experimental PED pattern with a database containing sets of PED patterns of the expected phases.¹⁵

In this paper, we demonstrate that when a low electron dose (<5 e/Å²) is ensured, the collection of a series of PED zone-axis patterns is possible for LiBH₄ and that the diffracted intensities can be used for structure solution and complete structure refinement including determination of the positions of the H atoms. To our knowledge, this is the first example of an ab initio crystal structure determination of a lightweight hydride from submicrometer-sized crystallites by ED.

2. EXPERIMENTAL SECTION

LiBH₄ of 95% purity (hydrogen basis) was purchased from Fluka and used without additional purification. Synchrotron powder X-ray diffraction (XRD) confirmed its single-phase character.

The samples for the PED investigation were prepared by crushing LiBH₄ crystals under dry hexane and depositing a drop of the suspension on a holey carbon grid mounted on a copper support. The grid was then inserted into a TEM specimen holder. All operations

were carried out in a glovebox with an argon atmosphere purified from H₂O and O₂. The specimen holder was transported to the microscope under an argon atmosphere. PED patterns were taken on a Phillips CM20 microscope with a LaB₆ electron gun, equipped with a Spinning Star precession instrument and a CCD camera. All patterns were taken with a precession angle of 2.5°. Reflection intensities were extracted and merged using *ELD-TRIPLE*.¹⁶ Structure solution was performed using direct methods with *SIR2011*.¹⁷ Structure refinement was performed with *JANA2006*.¹⁸

3. RESULTS

PED patterns of LiBH₄ were taken from many different crystallites of submicrometer size. The crystals were all very similar in size and in electron transparency, producing very low contrast, so, initially, we assume that they are comparably thin. All PED patterns were taken under the same experimental conditions, with a completely spread beam (instrumental limit) with 0.5 s exposure time, thus ensuring that all patterns were made with equivalent exposures. Because the electron-beam damage does not allow continuous operation on the same crystallite, eight zone-axis patterns were obtained from eight different crystallites (Figure 1, top). Indexing of the PED patterns reveals an orthorhombic unit cell with approximate cell parameters $a = 7.2$ Å, $b = 4.4$ Å, and $c = 6.8$ Å and $hk0$ ($h = 2n$) and $0kl$ ($k + l = 2n$) as the only reflection conditions, which corresponds only to the extinction symbol $Pn-a$, with $Pnma$ as

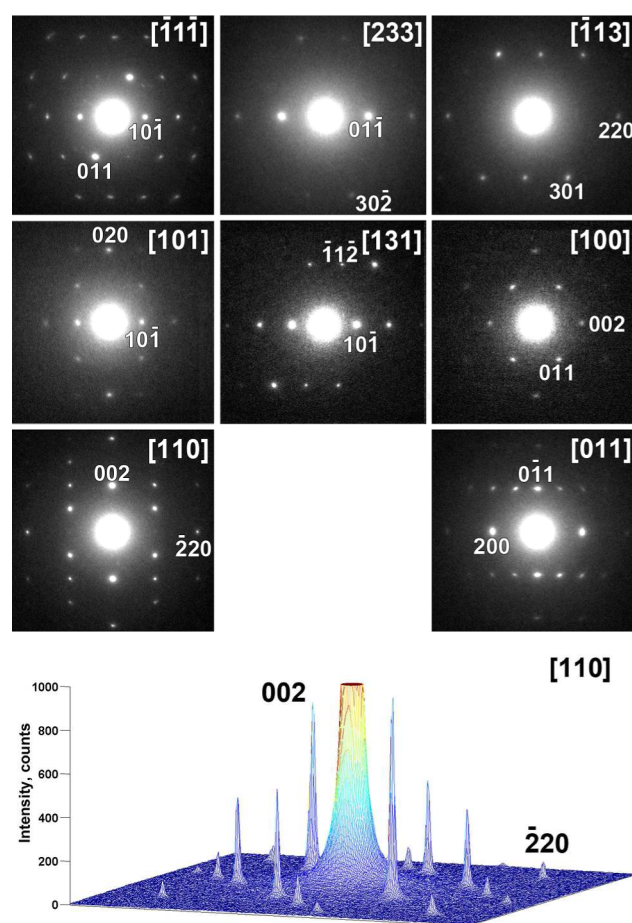


Figure 1. Top: PED patterns of LiBH₄. Bottom: intensity distribution on the [110] PED pattern. Note the absence of the forbidden reflections $hk0$ ($h \neq 2n$) and $00l$ ($l \neq 2n$), demonstrating largely kinematical diffraction.

the most symmetric space group, in agreement with the room temperature LiBH_4 structure determined by XRD.¹⁹

The diffraction intensities were extracted from each PED pattern. Although the extremely weak electron beam and short exposure times yielded only a moderate signal-to-noise ratio, the intensities of 411 reflections could be collected. The bottom of Figure 1 demonstrates a typical intensity distribution, showing that the intensities can be reliably quantified. The kinematical character of the PED pattern is proven by the absence of the kinematically forbidden reflections $hk0$ ($h \neq 2n$) and $00l$ ($l \neq 2n$). The correspondence between the diffracted intensities and the Laue symmetry was verified by symmetry averaging for every PED pattern, which leads to reliability factors R_{sym} of 5–13% (listed in Table S1 in the Supporting Information, together with the number of measured and symmetry-unique reflections).

The reflections from different 2D patterns were merged into one 3D set, assuming unit-scale factors due to equal beam intensity and exposure time. For structure solution, this assumption is valid because it has been shown in the literature that, at this step, it is sufficient simply to partition the reflections in three sets (strong, medium, and weak) to achieve a valid solution;²⁰ in the subsequent refinement, the scale factors will be refinable parameters. The final set of 115 unique observable reflections has been corrected with the geometrical correction factor

$$C_{\text{geom}} = g \sqrt{1 - \left(\frac{g}{2R}\right)^2}$$

where g is the reciprocal lattice vector and R is the radius of the Laue circle.²¹ The reflection list was used as input data for direct methods (coverage: 53% of the expected reflections above 1 Å and 19% down to 0.5 Å). Direct methods revealed the correct positions of the Li and B atoms (Table S2 in the Supporting Information) with $R_F = 21.5\%$. The H atoms were then located by defining rigid tetrahedra around the B atoms with $d(\text{B-H}) = 1.14$ Å and refining the x and y coordinates of the center of the tetrahedron and the rotation angle normal to the mirror plane (all other degrees of freedom are fixed by symmetry). Together with the x and y coordinates of the Li atoms and one overall atomic displacement parameter (ADP), this gives a total of six variables. The refinement was performed against 126 observed reflections [$(\sin \theta)/\lambda \leq 0.6$, i.e., $d \geq 0.83$ Å, 98 independent reflections] using separate refineable scale factors for each PED pattern. This first refined model was already close to the LiBH_4 structure from XRD, with the principal discrepancy being an 11.2° rotation of the BH_4 tetrahedra around the b axis with respect to the literature structure.¹⁹ As a final step, the two-beam correction for dynamical scattering was introduced using the Blackman formula:²²

$$C_{\text{Blackman}} = A_g \int_0^{A_g} J_0(2x) dx$$

where J_0 is the zero-order Bessel function, $A_g = \pi t/\xi_g$, t is the thickness of the crystallite, and $\xi_g \sim 1/|F_g|$ is the extinction distance for the reflection g with the structure factor F_g . The structure factors were calculated from the refined model, assuming that it is already quite close to the real structure. The reliability factors were calculated for different thicknesses of the crystals, and the lowest R factor was achieved for an effective thickness of 100 nm. The dynamical correction improved the

reliability factor R_F to 18.9% and brought the rotation angle of the BH_4 tetrahedra [$7(2)^\circ$] closer to its nominal value (nearly 0°). The isotropic overall ADP was refined to $0.051(8)$ Å², a reasonable value for a structure consisting of such light elements. The obtained atomic coordinates are very close to those calculated from single-crystal XRD,¹⁶ powder synchrotron XRD,²³ and neutron powder diffraction (NPD) data²⁴ (Table S2 in the Supporting Information) and provide reasonable interatomic distances [Table S3 in the Supporting Information, calculated with the unit cell parameters $a = 7.1900(7)$ Å, $b = 4.4447(4)$ Å, and $c = 6.8135(7)$ Å, obtained from synchrotron powder XRD data at room temperature²³]. The correspondence between the experimental structure amplitudes and the kinematically calculated amplitudes is shown in Figure 2, top. The list of the observed and calculated structure amplitudes is given in Table S4 in the Supporting Information. The refined structure is shown in Figure 2, bottom.

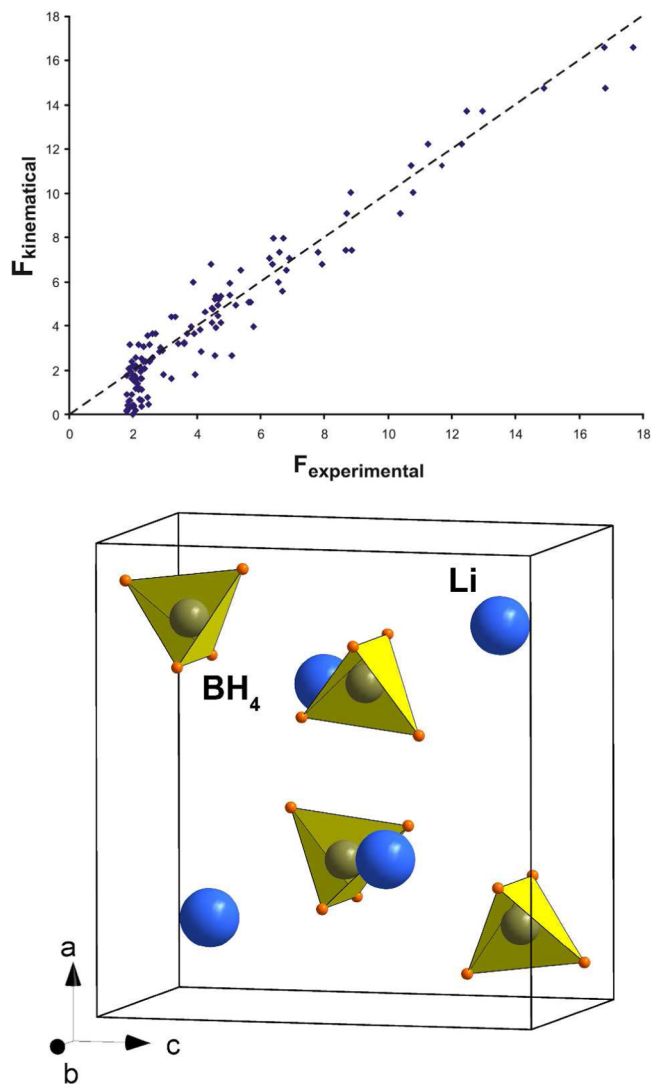


Figure 2. Top: Plot of the kinematically calculated structure amplitudes versus the experimental PED structure amplitudes after correction with the Lorentz factor and Blackman formula. Bottom: LiBH_4 structure as refined from the PED data.

4. DISCUSSION

The LiBH_4 structure as refined from PED data demonstrates a surprisingly good correspondence with the results from other diffraction methods, especially taking into account the limited amount of measured reflections and the low signal-to-noise ratio. Even at such unfavorable experimental conditions, the obtained reliability factor of $\sim 19\%$ is noticeably lower than the R factors of 25–30% typically accepted for PED structure refinements. Correcting for dynamic scattering improves the results, but not drastically; structures containing only low Z elements, such as lightweight complex hydrides, suffer much less from dynamic scattering. In this paper, it is shown that PED can be used directly for the crystal structure determination of lightweight complex hydrides. Apart from the possibility of determining structures from submicrometer areas, an additional advantage of PED compared with XRD is the greater sensitivity for locating the hydrogen positions. The electrostatic potential in the center of an atom (as is relevant for PED) is proportional to $Z^{0.8}$, while the electron density (as is relevant for XRD) is proportional to $Z^{1.25}$.²⁵ This means that the positions of light elements in the presence of heavier ones are better detectable from PED data than from XRD data. In the case of LiBH_4 , with $Z = 3, 5,$ and 1 for Li, B, and H atoms, respectively, the contrast ratio is $w = (Z_{\text{light}}/Z_{\text{heavy}})^{0.7} = 0.38$ for PED, whereas it is 0.18 for XRD. In PED experiments, the Fourier maps of the scattering density might be deteriorated because of the relatively low number of reflections, but using the rigid-body approximation (especially for borohydrides) is a useful tool to improve the precision of the location of the H atoms.

In conclusion, we have demonstrated that the low stability of lightweight complex hydrides toward the electron beam is not an obstacle for the collection of quantitative ED data. Even for one of the lightest known complex hydrides LiBH_4 , a complete structure solution can be performed using only PED data. With this technique, the crystallographic and structural information can be retrieved from submicrometer-sized particles. This provides new possibilities for the structural investigation of composite hydrogen-storage materials based on lightweight complex hydrides. Until now, such studies were mostly limited to elaborate studies by XRD and NPD.²⁶

■ ASSOCIATED CONTENT

■ Supporting Information

Zone-axis patterns used for the collection of quantitative diffraction data, their symmetry averaging reliability factors, and number of reflections, relative atom coordinates of LiBH_4 obtained in this work compared with literature data, selected interatomic distances, and list of the observed F_o and kinematically calculated F_k structure amplitudes used in the refinement. This material is available free of charge via the Internet at <http://pubs.acs.org>.

■ AUTHOR INFORMATION

Corresponding Author

*E-mail: joke.hadermann@ua.ac.be.

Author Contributions

The manuscript was written through contributions of all authors.

Notes

The authors declare no competing financial interest.

■ ACKNOWLEDGMENTS

This research received financial support from the University of Antwerp through a BOF-NOI grant, from the Flanders Research Foundation (Grant FWOG.0184.09N), and from ERC Grant 246791-COUNTATOMS.

■ REFERENCES

- (1) (a) Eberle, U.; Felderhof, M.; Schüth, F. *Angew. Chem., Int. Ed.* **2009**, *48*, 6608. (b) Sakintunaa, B.; Lamari-Darkrim, F.; Hirscher, M. *Int. J. Hydrogen Energy* **2007**, *32*, 1121.
- (2) Züttel, A.; Rentsch, S.; Fischer, P.; Wenger, P.; Sudan, P.; Mauron, Ph.; Emmenegger, Ch. *J. Alloys Compd.* **2003**, *356–357*, 515.
- (3) Li, C.; Peng, P.; Zhou, D. W.; Wan, L. *Int. J. Hydrogen Energy* **2011**, *36*, 14512.
- (4) (a) Vajo, J. J.; Skeith, S. L.; Mertens, F. *J. Phys. Chem. B* **2005**, *109*, 3719. (b) Vajo, J. J.; Salguero, T. T.; Gross, A. F.; Skeith, S. L.; Olson, G. L. *J. Alloys Compd.* **2007**, *446*, 409.
- (5) (a) Bogdanovic, B.; Schwickardi, M. *J. Alloys Compd.* **1997**, *253–254*, 1. (b) Zaluski, L.; Zaluska, A.; Ström-Olsen, J. O. *J. Alloys Compd.* **1999**, *290*, 71. (c) Bogdanovic, B.; Felderhoff, M.; Kaskel, S.; Pommerin, A.; Schlichte, K.; Schüth, F. *Adv. Mater.* **2003**, *15*, 1012.
- (6) Ishikawa, R.; Okunishi, E.; Sawada, H.; Kondo, Y.; Hosokawa, F.; Abe, E. *Nat. Mater.* **2011**, *10*, 278.
- (7) Williams, D. B.; Carter, C. B. *Transmission Electron Microscopy. A Textbook for Materials Science*; Plenum Publishing Corp.: New York, 2004; Vol. 1, p 64.
- (8) Vullum, P. E.; Pitt, M. P.; Walmsley, J. C.; Hauback, B.; Holmestad, R. *J. Alloys Compd.* **2011**, *509*, 281.
- (9) Egerton, R.; Li, P.; Malac, M. *Micron* **2004**, *35*, 399.
- (10) (a) Andrei, C. M.; Walmsley, J. C.; Brinks, H. W.; Holmestad, R.; Srinivasan, S. S.; Jensen, C. M.; Hauback, B. C. *Appl. Phys. A: Mater. Sci. Process.* **2005**, *80*, 709. (b) Felderhoff, M.; Klementiev, K.; Grünert, W.; Spliethoff, B.; Tesche, B.; Bellosta von Colbe, J. M.; Bogdanovic, B.; Härtel, M.; Pommerin, A.; Schüth, F.; Weidenthaler, C. *Phys. Chem. Chem. Phys.* **2004**, *6*, 4369.
- (11) (a) Gemmi, M.; Zou, X.; Hovmuller, S.; Migliori, A.; Vennstrom, M.; Andersson, Y. *Acta Crystallogr., Sect. A* **2003**, *59*, 117. (b) Gjønnnes, J.; Hansen, W.; Berg, B. F.; Runde, P.; Cheng, Y. F.; Gjønnnes, K.; Dorset, D. L.; Gilmore, C. J. *Acta Crystallogr., Sect. A* **1998**, *54*, 306. (c) Own, C. S.; Sinkler, W.; Marks, L. D. *Ultramicroscopy* **2006**, *106*, 114. (d) Kverneland, A.; Hansen, V.; Vincent, R.; Gjønnnes, K.; Gjønnnes, J. *Ultramicroscopy* **2006**, *106*, 492. (e) Vincent, R.; Midgley, P. A. *Ultramicroscopy* **1994**, *53*, 271.
- (12) Hadermann, J.; Abakumov, A. M.; Turner, S.; Hafideddine, Z.; Khasanova, N. R.; Antipov, E. V.; Van Tendeloo, G. *Chem. Mater.* **2011**, *23*, 3540.
- (13) Sedlmaier, S. J.; Mugnaioli, E.; Oeckler, O.; Kolb, U.; Schnick, W. *Chemistry* **2011**, *17*, 11258.
- (14) Kverneland, A.; Hansen, V.; Vincent, R.; Gjønnnes, K.; Gjønnnes, J. *Ultramicroscopy* **2006**, *106*, 492.
- (15) Moeck, P.; Rouvimov, S.; Rauch, E. F.; Véron, M.; Kirmse, H.; Häusler, I.; Neumann, W.; Bultreys, D.; Maniette, Y.; Nicolopoulos, S. *Cryst. Res. Technol.* **2011**, *46*, 589.
- (16) Zou, X.; Sukharev, Y.; Hovmöller, S. *Ultramicroscopy* **1993**, *52*, 436.
- (17) Burla, M.; Camalli, M.; Barrozzini, B.; Cascarano, G. L.; Giacobozzo, C.; Polidori, G.; Spagna, R. *J. Appl. Crystallogr.* **2003**, *36*, 1103.
- (18) Petricek, V.; Dusek, M. *JANA2000: Programs for Modulated and Composite Crystals*; Institute of Physics: Praha, 2000.
- (19) Filinchuk, Y.; Chernyshov, D.; Cerny, R. *J. Phys. Chem. C* **2008**, *112*, 10579.
- (20) Klein, H.; David, J. *Acta Crystallogr., Sect. A* **2011**, *67*, 297.
- (21) Gemmi, M.; Nicolopoulos, S. *Ultramicroscopy* **2007**, *107*, 483.
- (22) Gjønnnes, K.; Cheng, Y.; Berg, B. S.; Hansen, V. *Acta Crystallogr., Sect. A* **1998**, *54*, 102.
- (23) Soulie, J. P.; Renaudin, G.; Cerny, R.; Yvon, K. *J. Alloys Compd.* **2002**, *1*, 1–123.

- (24) Hartman, M. R.; Rush, J. J.; Udovic, T. J.; Bowman, R. C.; Hwang, S. Y. *J. Solid State Chem.* **2007**, *180*, 1298–1305.
- (25) Vainshtein, B. K. *Structure analysis by electron diffraction*; Pergamon Press: Oxford, U.K., 1964.
- (26) Černý, R.; Filinchuk, Y. Z. *Kristallogr.* **2011**, *226*, 882.